THE ASTROPHYSICAL JOURNAL, 469:508–518, 1996 October 1

HUBBLE SPACE TELESCOPE OBSERVATIONS OF GIANT ARCS: HIGH-RESOLUTION IMAGING OF DISTANT FIELD GALAXIES[1]

IAN SMAIL,[2] ALAN DRESSLER,[2] JEAN-PAUL KNEIB,[3] RICHARD S. ELLIS,[3] WARRICK J. COUCH,[4]
RAY M. SHARPLES,[5] AND AUGUSTUS OEMLER, JR.[6]

Received 1995 March 17; accepted 1996 April 10

ABSTRACT

We present *Hubble Space Telescope* (*HST*) imaging of eight spectroscopically confirmed giant arcs, pairs, and arclets. These objects have all been studied extensively from the ground, and we demonstrate the unique advantages of *HST* imaging in the study of such features by a critical comparison of our data with the previous observations. In particular, we present new estimates of the core radii of two clusters (Cl 0024+16, A370) determined from lensed features that are identifiable in our *HST* images. Although our *HST* observations include both pre- and postrefurbishment images, the depth of the exposures guarantees that the majority of the arcs are detected with diffraction-limited resolution. A number of the objects in our sample are multiply imaged, and we illustrate the ease of identification of such features when working at high resolution. We discuss the morphological and size information on these distant field galaxies in the light of *HST* studies of lower redshift samples. We suggest that the dominant population of star-forming galaxies at $z \sim 1$ is a factor of 1.5–2 times smaller in size than the equivalent population in the local field. This implies either a considerable evolution in the sizes of star-forming galaxies within the last $\sim$10 Gyr or a shift in the relative space densities of massive and dwarf star-forming systems over the same timescale.

Subject headings: galaxies: clusters: general — galaxies: photometry — gravitational lensing

1. INTRODUCTION

The study of galaxy evolution using luminosities, angular sizes, or other morphological characteristics of the galaxies is a standard technique in observational cosmology. Until recently, however, the limitations of observing from the ground have meant that the crucial morphological information has been unavailable for the most distant objects. This has been one of the major restrictions on the study of "normal" galaxies at high redshift. With the refurbishment of the *Hubble Space Telescope* (*HST*), we are finally in a position to remove this obstacle. While *HST* has been used to study large samples of *cluster* galaxies at moderate redshifts (Dressler et al. 1994; Couch et al. 1994), similar sized samples of moderate- and high-redshift ($z \gtrsim 0.5$) field galaxies with spectroscopic identifications have been slower to appear.

Interest in faint galaxy evolution has centered on the problem of the "excess" faint galaxy population apparent in deep optical counts (Ellis 1994). While the cumulative surface density of galaxies exceeds the extrapolations from local populations (the no-evolution model), their redshift distribution is apparently consistent, at least to $B \sim 24$, $I \sim 22$ with the same no-evolution model (Glazebrook et al. 1995; Lilly 1993; Tresse et al. 1993). Gravitational lensing studies of the median redshift of yet fainter samples, $B \sim 27$, indicate that the no-evolution model is still an adequate description at this depth (Kneib et al. 1994, 1995b; Smail, Ellis, & Fitchett 1994).

The key to understanding these results may come from morphological studies of the faint field population. A first attempt at this was made by Giraud (1992), who used ground-based imaging taken in sub-arcsecond seeing to study the morphologies of a small sample of blue $I < 23$ field galaxies. He broke his sample into three broad categories: compact galaxies with extended halos (33% of the sample), extended irregular sources (50%), and multiple or merging objects (17%). He concluded that the star formation responsible for the blue colors of the faint field population arose from a variety of different physical mechanisms, rather than a single class of objects. A similarly simple scheme was used by Glazebrook et al. (1996) and Driver et al. (1995) in their morphologically classified number counts to $I < 22$ and $I < 24$, respectively, using the postrefurbishment *HST* data. With just three categories (spirals, spheroidals, and irregulars), they found that those objects classified as either spiral or spheroidal had counts consistent with a nonevolving slope, while the irregular sample had much steeper counts and would therefore dominate at fainter magnitudes. If this is the case, then additional information about this population and its characteristics at high redshift is necessary to obtain a coherent view of faint galaxy evolution. A categorization in terms of scale size may be a useful tool to study the evolution of distant field galaxies, especially the growth of spiral disks if such an event is visible. The use of such information to distinguish between various evolutionary models is discussed from a theoretical basis by Im et al. (1996). Using prerefurbishment *HST* Medium Deep Survey (MDS) data, Mutz et al. (1994) studied the scale sizes of galaxy images as a function of redshift. They find that their disk galaxies have intrinsic sizes similar to those of local bright spirals, although their data are also consistent with size evolution of $(1 + z)^{-1}$.

[1] Based on observations with the NASA/ESA *Hubble Space Telescope*, obtained at the Space Telescope Science Institute, which is operated by the Association of Universities for Research in Astronomy, Inc., under NASA contract NAS 5-26555.

[2] The Observatories of the Carnegie Institution of Washington, 813 Santa Barbara Street, Pasadena, CA 91101-1292.
[3] Institute of Astronomy, Madingley Road, Cambridge CB3 0HA, UK.
[4] School of Physics, University of NSW, Sydney 2052, NSW Australia.
[5] Department of Physics, University of Durham, South Rd, Durham DH1 3LE, UK.
[6] Yale Observatory, New Haven, CT 06511.

Either way, there is only weak evidence for size evolution of spiral disks over the last ~ 3 Gyr.

Unfortunately, the Mutz et al. (1994) sample probes only to $I \sim 21$, corresponding to a median depth of $z \sim 0.2$, and while the Glazebrook et al. (1996) and Driver et al. (1995) samples are deeper, they have only statistical redshift information. Ideally, we would like to study the distributions of morphology and size at earlier times to observe the changes in the nature of the faint field population responsible for the steep optical counts. Such a search is hampered, however, by the faintness of these distant galaxies, which makes redshift identification extremely time consuming. Thus, at high redshift we are constrained to study only the intrinsically brightest and hence possibly least representative objects. Gravitationally lensed features, in particular giant arcs, may offer an alternative approach to study a small sample of "normal" distant galaxies.

Giant arcs are formed by the serendipitous alignment of a massive, concentrated foreground cluster along our line of sight to a distant background galaxy. The strong deflection of the light paths to the distant galaxy result in our observing a highly distorted and magnified image of the source. The amplification of the source brings what would have been apparently very faint galaxies within the reach of modern spectrographs, enabling us to identify spectroscopically the source redshifts. Moreover, by combining the natural magnification of the source by the lensing cluster with the high-resolution imaging available with *HST*, we can gain a detailed insight into the morphologies and sizes of a small sample of very distant field galaxies. The lensing process induces extreme distortions in the image of the distant galaxy, and to reconstruct accurately the complete source morphologies would require detailed numerical lens inversions of each of the lensing clusters (e.g., Wallington, Kochanek, & Koo 1995). Nevertheless, we believe that sufficient information is available from just the arc images to tackle the questions of the broad morphologies and sizes of $z \gtrsim 1$ field galaxies with this data set. We can determine the scale sizes of the sources to search for new populations of compact galaxies (e.g., Miralda-Escudé & Fort 1993) and also use the structure in the arcs to look at the clumpiness of the star formation in these very distant galaxies. In the discussion below, we compare the predominantly blue arc sources with samples of the dominant local star-forming field galaxies: spirals. These local samples are observed mostly in blue optical bands, and thus they are reasonably matched to our data.

When using arcs to study the sizes of faint galaxies, we have to understand both the gross properties of the lensing clusters (see § 4) and also the role of selection biases in the original discovery of the arcs. All the arcs discussed here were discovered in optical passbands (sampling the blue and ultraviolet restframe) and are effectively surface brightness selected. It has been demonstrated, however, that these arcs have optical and optical-infrared colors compatible with the bulk of the faint field population (Smail et al. 1993) when allowance is made for the lensing amplification. Thus, at least from their colors, there is no evidence for selection biases peculiar to the lensing process, and the arcs appear to be a representative sample of the high-redshift field galaxy population.

If we wish to use the giant arcs to study the scale sizes of distant galaxies, we must also discuss the arc detection as a function of intrinsic source size. For the giant arcs used here, the high tangential amplification means there should be no bias against finding thick arcs formed from intrinsically large background sources (e.g., Wu & Hammer 1993). However, a bias may exist against identifying the gravitationally lensed images of compact sources. When strongly lensed, these sources do not appear as highly elongated and easily recognizable giant arcs, but rather as multiple, discrete images. These multiple image systems are difficult to identify in the crowded cluster core unless they have either extreme colors or internal structure that is visible in each of the multiple images (e.g., Smail et al. 1995a). We might, therefore, expect compact sources to be underrepresented in the current giant arc sample. In conclusion, we would expect to be able to derive a firm upper limit on the scale size distribution of distant galaxies from the study of the widths of giant arcs.

This paper presents high-resolution imaging of eight spectroscopically confirmed, high-redshift field galaxies. These galaxies appear as giant arcs, pairs, or arclets in the fields of moderate redshift clusters. Using *HST*, we have acquired deep optical imaging of these arcs at 0.″1 resolution. Thus, we have detailed views of these galaxies at rest-frame ultraviolet-blue wavelengths on spatial scales of $\sim 0.5\, h^{-1}$ kpc.[7] The bulk of the observations of lensed features presented here has not been discussed previously, and we show a number of gravitationally lensed objects uncovered with *HST* that have important consequences for the modeling of the cluster mass distributions.

2. OBSERVATIONS AND REDUCTION

Four of the five clusters presented (A370, AC 114, Cl 0024+16, A2218) were observed for studies of galaxy evolution in distant clusters (Dressler et al. 1994; Couch et al. 1994). The presence of giant arcs in these fields is purely serendipitous and in some respects reflects the prevalence of such features in these rich, moderate-redshift clusters. The fifth cluster, Cl 2244−02 was observed in Cycle-2 to study the arc present in the cluster and these images were retrieved from the STScI archive (Prop. 2801, Principle Investigator R. E. Sterner).

The majority of the clusters discussed here were observed with prerefurbishment WFC-1 on *HST* (Table 1). The uncorrected aberrations of the telescope's primary mirror led to a very extended point-spread function (PSF) in WFC-1 images. Roughly 20% of the incident light was contained in a diffraction-limited core, with the remaining 80% lying in an extended halo. By virtue of the relatively long integration times of our exposures, we obtain strong detections of the majority of the arcs. Thus, we have a high enough signal-to-noise ratio to use the information available in the diffraction-limited core of the PSF to study qualitatively the internal structures of the arcs on scales of $\sim 0.''1$, without resorting to image restoration techniques. Thus, *HST* provides the crucial factor of $\gtrsim 4$–5 improvement in resolution over the best ground-based imaging (e.g., Kneib et al. 1993) necessary for a detailed examination of these distant galaxies. However, when we study the light profiles of the arc sources, rather than their internal morphologies, we must take account of the smearing introduced by the extended halo of the PSF. To measure half-light radii

[7] We use $h = H_0/100$ km s^{-1} Mpc^{-1} and $q_0 = 0.5$ unless otherwise stated.

TABLE 1

HST OBSERVATIONS OF ARC CLUSTERS

Cluster	Date	Instrument	$\alpha(2000)^a$	$\delta(2000)^b$	t_{exp} (s)	Filter
AC 114	1991 Nov	WFC-1	22 58 47.0	−34 48 13.5	15300	F555W
	1991 Nov	WFC-1			13800	F814W
Cl 2244−02.....	1992 Apr	WFC-1	22 47 12.2	−02 05 38.8	8100	F555W
Cl 0024+16.....	1992 Sep	WFC-1	00 26 32.2	+17 09 54.9	24300	F702W
A370	1992 Nov	WFC-1	02 37 21.9	−01 47 15.5	17600	F702W
A2218.....	1994 Sep	WFPC-2	16 35 57.0	+66 12 38.0	6500	F702W

[a] In units of hours, minutes, seconds.
[b] In units of degrees, arcminutes, arcseconds.

(r_{hl}) for the arcs, we have chosen to correct for the extended PSF of the WFC-1 images by deconvolving our frames. Therefore, the frames were processed by deconvolving for 40 iterations of the Lucy-Richardson algorithm using model PSFs created with TINYTIM (Krist 1992). This procedure has been tested extensively tested by Windhorst et al. (1994), who report that it is adequate for restoring a galaxy's average light profile. To measure the half-light radii of the arcs, we extract profiles through the arcs, orthogonal to the local shear direction indicated by the arc's shape. These profiles are effectively one-dimensional slices through the source, and they must be corrected by weighting radially the profile to reflect the two-dimensional geometry of the source, to give standard half-light radii, with typical measurement errors of ∼0″.1. Table 2 gives half-light radii for the arcs measured from our *HST* frames. It should be noted that for all arcs, except A5 in A370, we detect the source out to $\gtrsim 3$ times the measured half-light radius. To estimate our resolution limit, we have analyzed similarly processed stars from our images, showing that the resolution limit of *HST* is approximately $r_{hl} \sim 0''.1$–$0''.2$. Thus, *HST* resolves well all but one arc, Cl 2244−02, in our sample.

3. RESULTS

We discuss lensed features in four of the clusters from our sample (Cl 0024+16, A370, A2218, Cl 2244−02), where the *HST* data contribute significant new information compared to published ground-based studies. When the background source has internal structure, the improved resolution available from *HST* confirms graphically the lensed nature of the giant arcs. Some of the *HST* observations of lensed features used here have been discussed previously, including AC 114 in Smail et al. (1995a) and the arclet population in A2218 in Kneib et al. (1995b), and the WFC-1 image of Cl 0024+16 was commented on by Kassiola et al. (1994, and Kassiola, Kovner, & Dantel-Fort (1995).

3.1. Cl 0024+16; $z_{cl} = 0.39$

The arcs in Cl 0024+16 were originally noted by Koo (1988), and the cluster has been studied subsequently by the Toulouse group. However, their deep spectroscopy has only been able to place limits on the arc's redshift, $1 \lesssim z_{arc} \lesssim 2$ (Mellier et al. 1991). We show the three main sections A–C of the arc in Figure 1. Unfortunately, all three sections are contaminated by projected bright galaxies. The difficulty of removing this contamination is illustrated by the disagreement between Kassiola et al. (1995) and Wallington et al. (1995) over which components of the arcs A–C are multiply imaged using ground-based imaging. The fourth arc, D, has been proposed as a counter arc to A, B, and C on a number of occasions, and while Worthey et al. (D. C. Koo 1994, private communication) were able to fit D qualitatively as a counterarc, most other groups have dismissed it when they could not recreate it easily in their adopted lensing models of the cluster (e.g., Kassiola, Kovner, & Fort 1992; Kassiola et al. 1995; Wallington et al. 1995).

The factor of $\gtrsim 5$ improvement in resolution with *HST* over the ground-based data makes the identification of the various multiply imaged components in all the arcs much less ambiguous. We see a bright elongated knot (marked as 2) in all four images A–D, surrounded by a low surface brightness halo (Fig. 1*a*). Closer inspection indicates that the knot comprises two peaks, with separations (A_2–D_2) of 1″.1, 0″.5, 0″.7, and 0″.6, roughly consistent with the relative lengths of the various arc components. In addition to this double peak, a fainter feature (marked as 3 in Fig. 1*b*) is visible also in all four arcs. The parities shown by these

TABLE 2

PHOTOMETRIC DATA ON SPECTROSCOPIC ARCS[a]

Arc	z_{cl}	z_{arc}	R	$(B-R)$	$(R-K)$	r_{hl}	Multiple
AC 114 (A0).....	0.31	0.639	21.3	1.37	2.0	0.78	N
A2218 (no. 359)	0.18	0.702	20.7	3.60	3.6	0.47	N
A370 (A0).....	0.37	0.725	19.1	1.97	4.1	0.54	N
A2218 (no. 289)	0.18	1.034	21.2	1.27	...	0.58	Y
Cl 0024+16 (C).....	0.39	≥1	22.8	0.7	3.3	0.78	Y
A370 (A5).....	0.37	1.306	21.3	1.05	2.9	0.39	N
AC 114 (S1/S2)	0.31	1.86	22.0	0.50	2.3	0.63	Y
Cl 2244−02	0.33	2.237	20.6	0.77	2.5	0.26	Y

[a] Basic photometric data on the spectroscopically confirmed lensed features in the *HST* fields. Data are taken from the compilations of Mellier et al. (1991), in addition to Kneib et al. (1993, 1995a), Pelló et al. (1992) and Smail et al. (1993). The last two columns give the half-light radii of the arc sources, r_{hl}, in arcseconds and whether multiple components are visible in the light distribution.

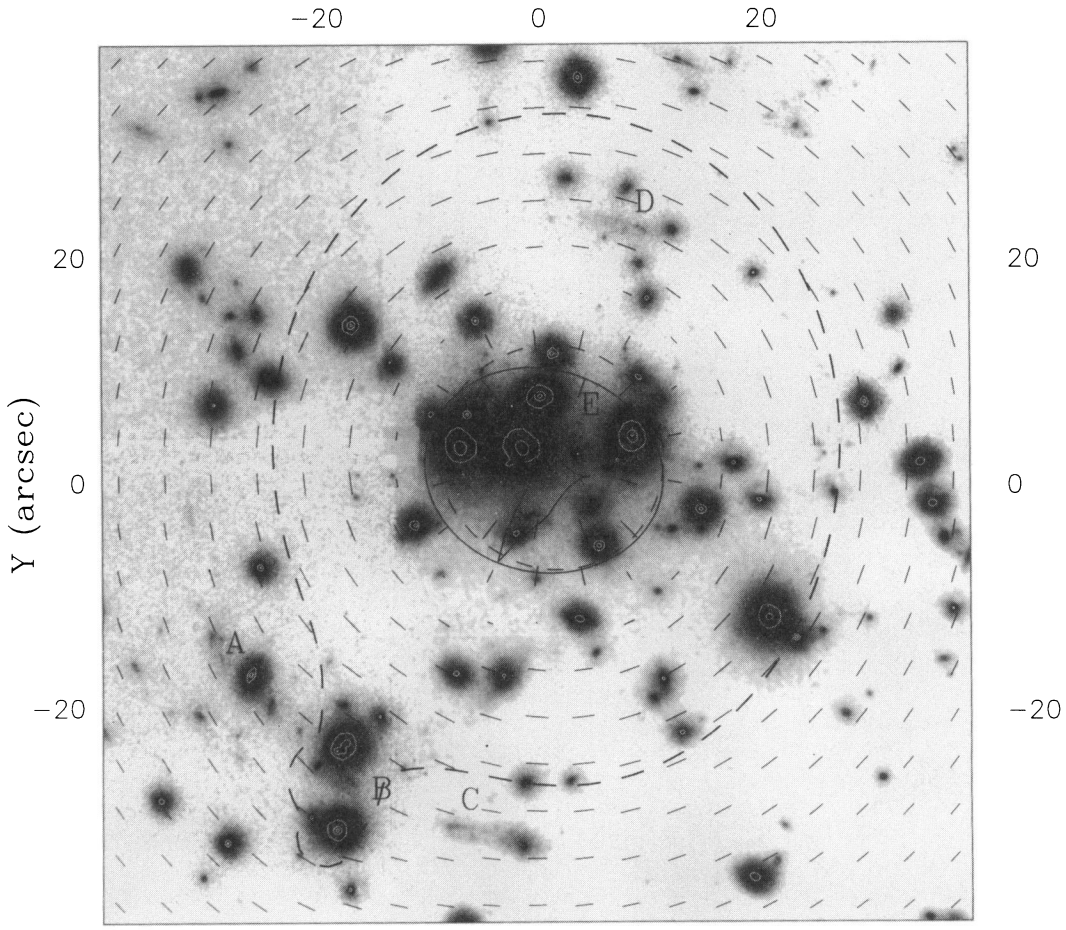

FIG. 1*a*

FIG. 1.—(*a*) The central region of our WFC-1 F702W image of Cl 0024+16 ($z_{cl} = 0.39$). The compact core of the cluster is easily visible, as are the four components of the arc. We overlay on this image the critical curves and the shear map from our lensing model of the cluster, see § 3.1. Using this model, we suggest tentatively that object E from Kassiola et al. (1992) may be the fifth image of the source. Unfortunately, E is too faint to be seen in the crowded cluster core in this frame, and we merely mark its approximate position. (*b*) An enlarged view of the four components of the arc, A–D. The morphological features which repeat between all the arc segments are shown, proving conclusively that component D is the counterarc to A–C. The images are 15″ × 15″ and have been smoothed with a Gaussian with a 0.″15 FWHM to reduce sky noise. Marked are the features discussed in the text using the naming scheme adopted by Kassiola and coworkers (Kassiola et al. 1992, 1995).

features in the individual arcs are consistent with the lensing hypothesis and indicate that D is a counterarc to A–C, a conclusion that is also supported by the spectroscopy of the four components, as stated in Mellier et al. (1991).

A counterarc such as D arises naturally in models of the triple arc A–C using a lensing potential with a small core radius and small ellipticity. To illustrate this, we have devised a simple lensing model for this cluster using one potential for the cluster and perturbations associated with the two bright galaxies near the arc component B. The technique and model potentials are the same as those used in Kneib et al. (1995a), and we fix the positions, orientations, and ellipticities of the singular potentials representing the perturbing galaxies to be those observed for their light distributions. Our model has eight free parameters; six for the cluster potential: position, ellipticity, position angle, core radius, and velocity dispersion; and one each for the velocity dispersions of the perturbing galaxies. We find a dispersion on the predicted positions of the peaks A_2–D_2 in the images of ∼0.″1–0.″2 for our best-fit model, with a slightly worse error for the fainter knot A_3–D_3 of ∼0.″2–0.″3. Thus, we claim that our best-fit model provides an adequate description of the arcs A–D. The characteristics of this model are a nearly circular mass, $\epsilon \sim 0.15 \pm 0.05$, with a major-axis angle within 10° of the direction to arc D and centered within 2″–3″ of the optical center of the cluster. For a source at $z_{arc} \sim 1.3$, the mass inside the radius of the arc is $M = (1.0 \pm 0.1) \times 10^{14}\ h^{-1}\ M_{\odot}$. The cluster has a core radius of $r_c \sim (20 \pm 5) h^{-1}$ kpc, comparable to those derived for other well-constrained cluster lenses (e.g., MS 2137−23, Mellier, Fort, & Kneib 1993; A370, this work). Thus, not only does the detailed morphology of D support its identification as a counterarc, but we are also able to reproduce its position and morphology easily using a simple model of the lensing cluster.

The small, but nonzero, core in our lens model means that we expect to see a fifth image of the source in the very center of the cluster. Unfortunately, the faintness of this image in the crowded cluster core means that we are unable to identify conclusively the fifth image via its morphology on our F702W exposure. However, the blue object E cataloged by Kassiola et al. (1992) in the cluster core fits the rough characteristics we predict for the fifth image, both in its position and surface brightness (we mark the approximate position of E in Fig. 1*a*). Thus, we suggest that object E (see Fig. 11*a* of Kassiola et al. 1992) is a good candidate

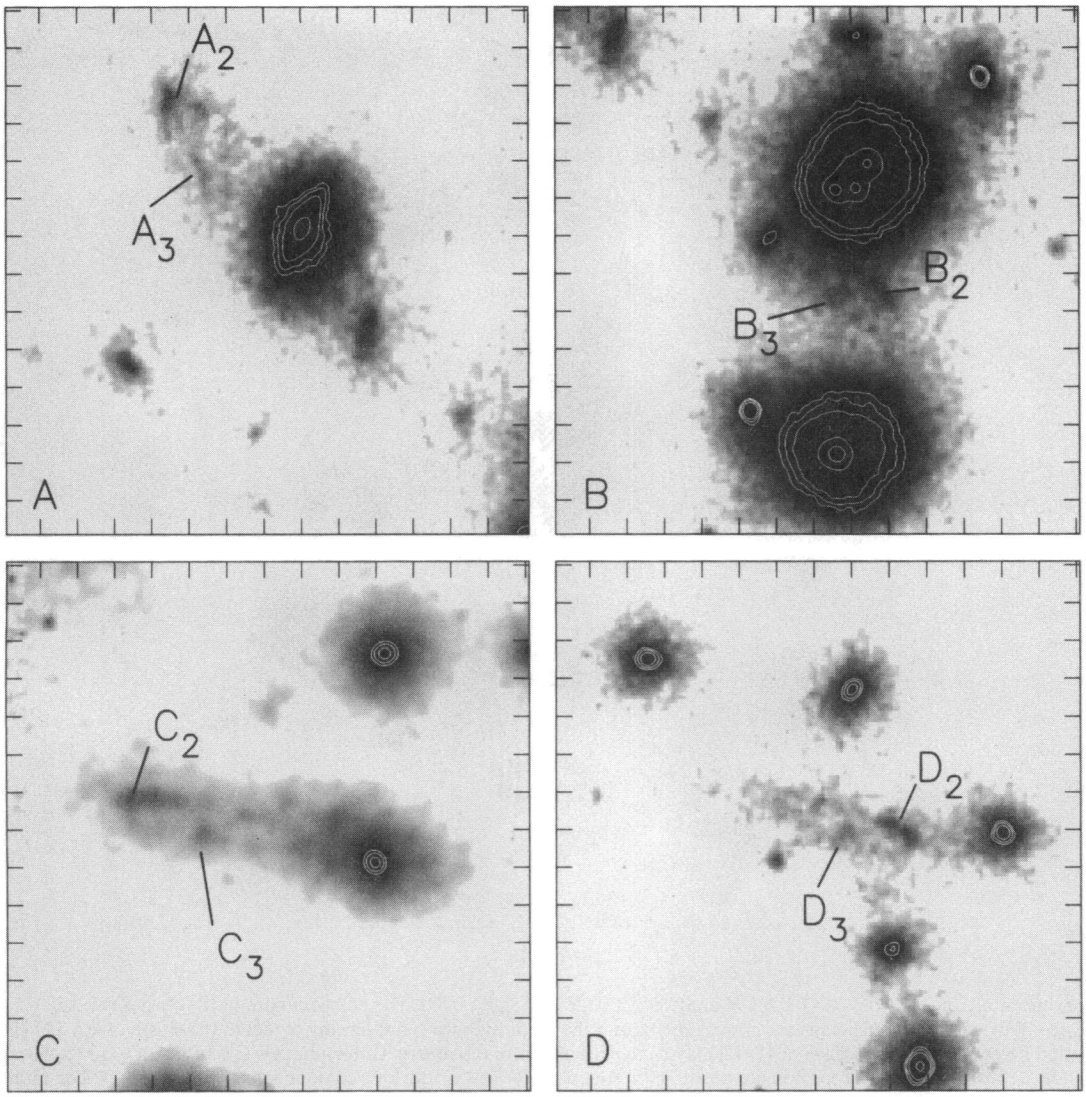

FIG. 1*b*

for the fifth image, allowing a direct confirmation of the core radius predicted by our lensing model.

3.2. A370; $z_{cl} = 0.37$

The giant arc, A0, in A370 was the first gravitationally lensed galaxy identified ($z_{arc} = 0.725$; Soucail et al. 1987). The optical-infrared colors and spectral properties of this arc are consistent with the source being a mid-type spiral (Table 2, Aragón-Salamanca & Ellis 1990). The arc is shown in Figure 2*a*; its highly elongated morphology implies that it consists of multiple images of a single source. With the exceptional seeing of their deep Canada-France-Hawaii Telescope (CFHT) images, Kneib et al. (1993) confirmed the multiply imaged hypothesis by identifying the breaks and peaks associated with the various images (Fig. 2*b*). However, they also concluded that the situation was more complex, as not all of the source is multiply imaged. In the Kneib et al. (1993) model, only the central P2–P4 are multiple images, with P1 and P5 being singly imaged regions of the source. Close scrutiny pf A0 (Fig. 2*b*) shows that fine structure is visible within P1, including an apparent bulge/nucleus and possibly faint spiral structure, suggesting morphological confirmation of the spiral nature of the source.

The extensive studies of the Toulouse group (Fort et al. 1988; Mellier et al. 1991; Kneib et al. 1993) have provided a number of other gravitationally lensed features in this cluster. These include the arclet, A5 ($z_{arc} = 1.306$, Fig. 2*c*), as well as a number of candidate multiply imaged sources. Among the latter features is the first object (B2–B4; Fig. 2*a*), whose redshift, $z_{arc} = 0.865$, has been determined by direct inversion of a lensing model of a cluster (Kneib et al. 1993). Unfortunately, these objects are too faint for us to measure reliable scale sizes from our current images, and so we will not discuss them further.

One feature visible on our WFC-1 image which has not been cataloged previously is a radial structure (R; Figs. 2*a*–2*b*): although 4".8 long, the faintness ($R \sim 22.9$) compared to the cD envelope and the fineness of this feature makes it invisible on even the superb CFHT images of the cluster (Kneib et al. 1993). We suggest that this feature represents a radial arc, formed by two images merging across the inner critical curve of the cluster, corresponding roughly to the core radius of the potential. Thus, the existence of a radial arc proves immediately that the potential is nonsingular. Furthermore, the position of R, lying between 20–30 h^{-1} kpc from the center of the southern D galaxy,

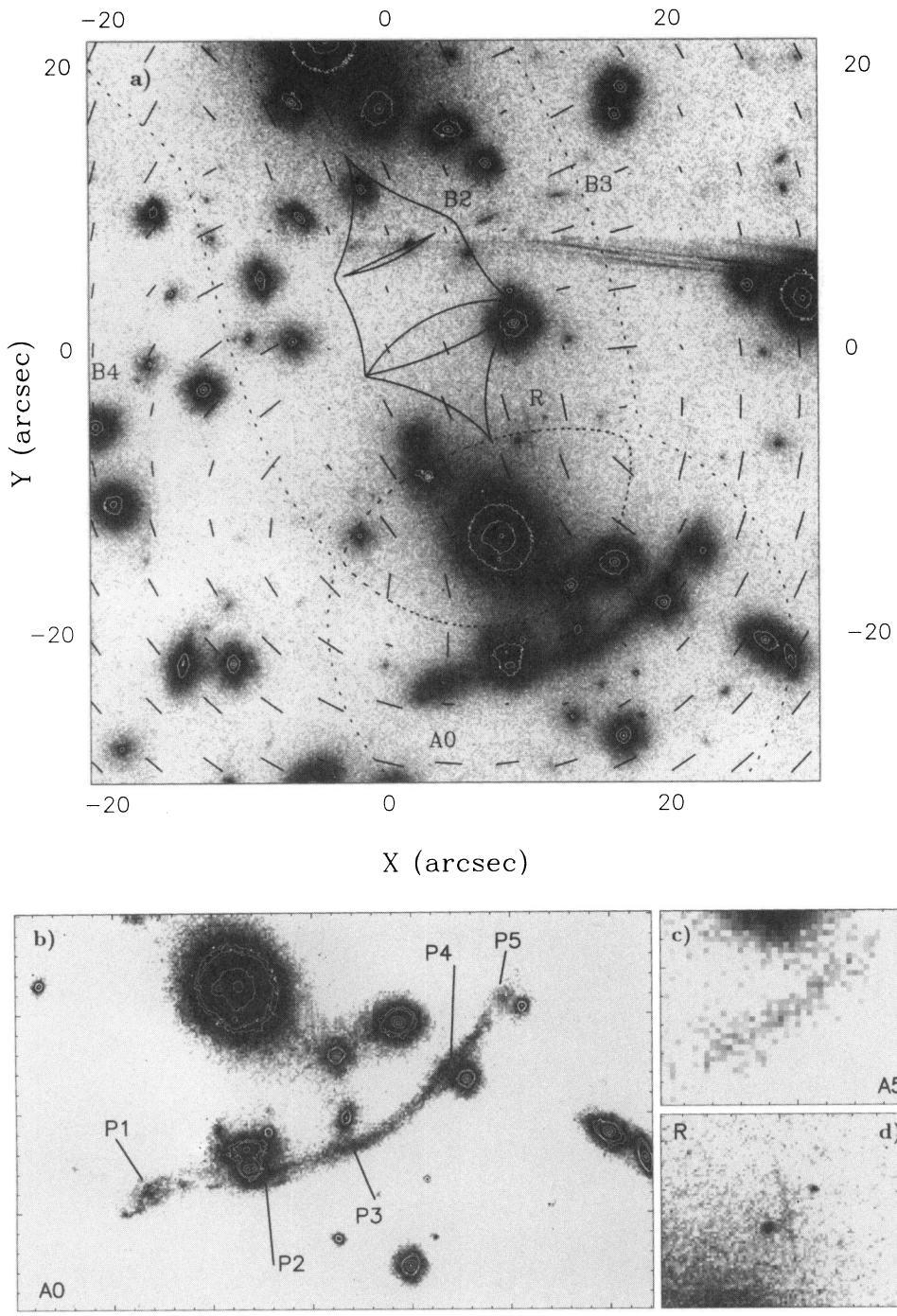

FIG. 2.—(*a*) The central section of the WFC-1 F702W image of A370 ($z_{cl} = 0.37$) showing the giant arc A0 ($z_{arc} = 0.725$). Also shown is the multiply imaged feature B2–B4 modeled by Kneib et al. (1993) and the newly discovered candidate radial arc, R (see also panel *d*). Using Kneib et al.'s cluster model, we estimate a redshift $z_{arc} = 1.3 \pm 0.2$ for the source of R. We show also the critical curves (*dashed lines*), caustics (*solid lines*), and shear field (*vectors*) appropriate for R. (*b*) A zoom on the giant arc A0 showing the two singly imaged regions P1 and P5 as well as the multiply imaged sections P2–P4. Notice the bulge and weak spiral structure visible in P1. The minor tick marks show 1″. (*c*) The featureless arclet A5 ($z_{arc} = 1.305$); again the minor tick marks are every 1″. (*d*) An enlarged view of the field around the candidate radial arc R; minor tick marks indicate 1″.

gives a crude estimate of the core size. We estimate, therefore, a core radius for the subclump around the southern D galaxy in A370 of $r_c \sim 25\ h^{-1}$ kpc. This is in agreement with the limit derived by Kneib et al. (1993) and is also similar to the values obtained from lensing analyses of other clusters, which give $r_c \lesssim 25$–$50\ h^{-1}$ kpc (see § 3.1).

Reassuringly, the lensing model of Kneib et al. (1993) that explains the multiply imaged system B2–B4 is also capable of fitting the radial arc with no modifications. The model predicts that the source is at $z_{arc} \sim 1.3 \pm 0.2$. We show the shear field predicted by the model and the critical curves in Figure 2*a*; as can be seen, R has the correct orientation for a radial arc and also straddles the inner critical curve of the lens, as expected. The model predicts also that this feature corresponds to two merging images from a five-image configuration. The three other images will have a similar

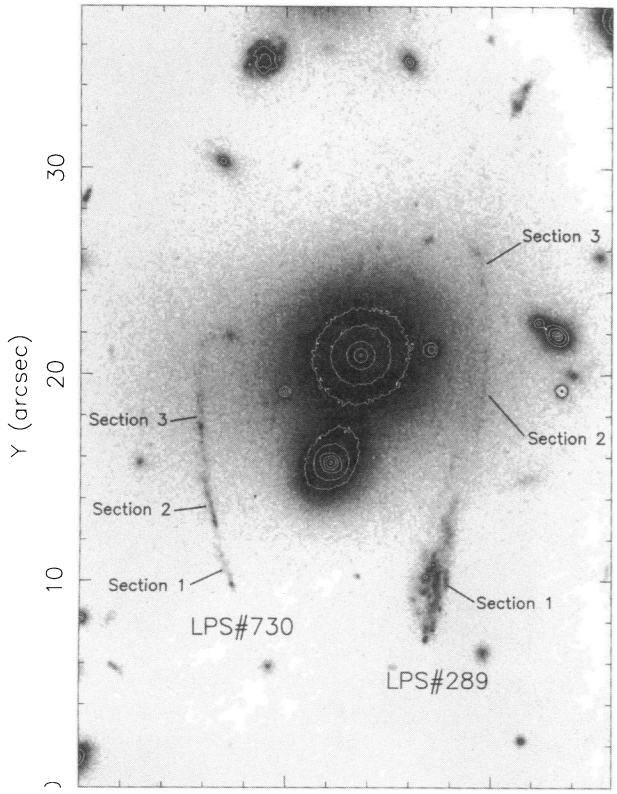

FIG. 3*a*

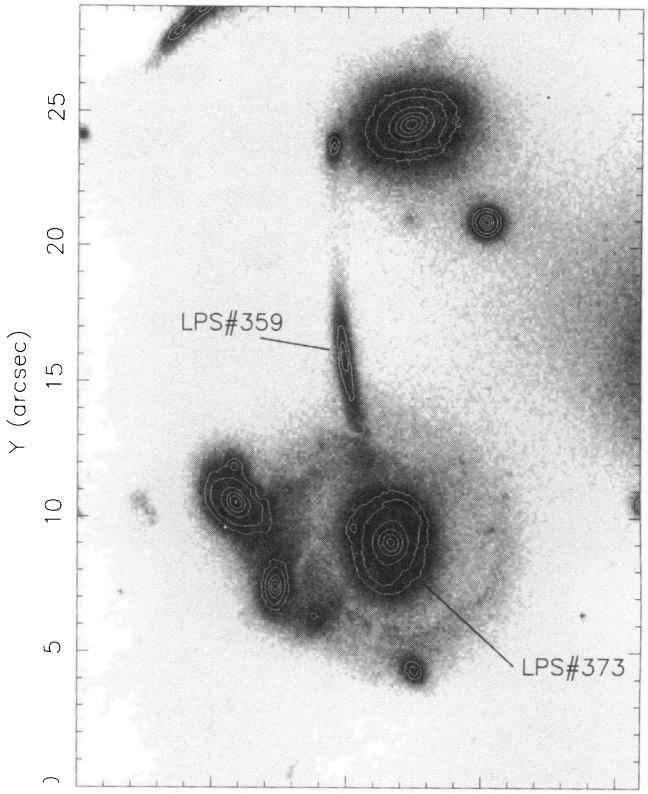

FIG. 3*b*

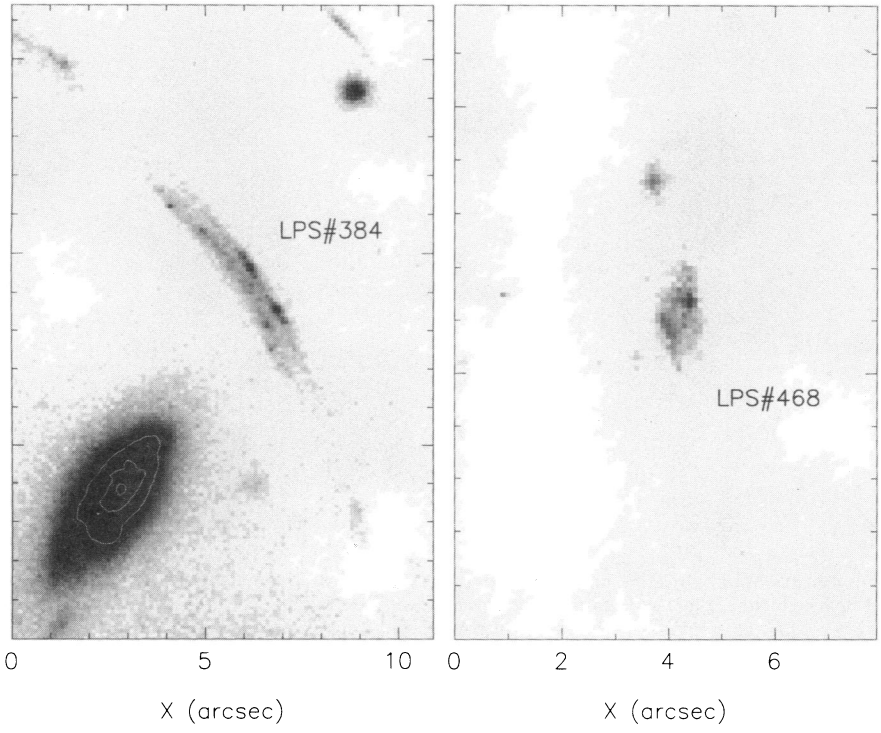

FIG. 3*c*

FIG. 3.—(*a*) The arc LPS 289 in A2218 ($z_{cl} = 0.18$). The arc has a spectroscopic redshift of $z_{arc} = 1.034$, and complex structure is visible in the main component (section 1). Sections 2 and 3 may be multiply imaged regions of the source. Also shown is the multiply imaged arc LPS 730, for which a redshift has not yet been measured. (*b*) The figure shows the Einstein ring proposed by Pelló et al. (1992) around galaxy LPS 373 in A2218. Weak spiral structure is visible within the ring, supporting our conclusion that it is associated with the central galaxy rather than a lensed feature. The red arc LPS 359 ($z_{arc} = 0.702$) shows little internal structure, consistent with an identification as a moderate redshift spheroidal system. (*c*) The left panel shows the candidate arc LPS 384, which Pelló et al. (1992) claimed to most likely be foreground of the cluster from weak spectroscopic evidence. The multiple nature of this arc is striking, and thus we claim that it arises from a background source lensed by the cluster core. The right panel has a transposed image of the counterarc (LPS 468) to LPS 384 showing similar internal structure to the main arc.

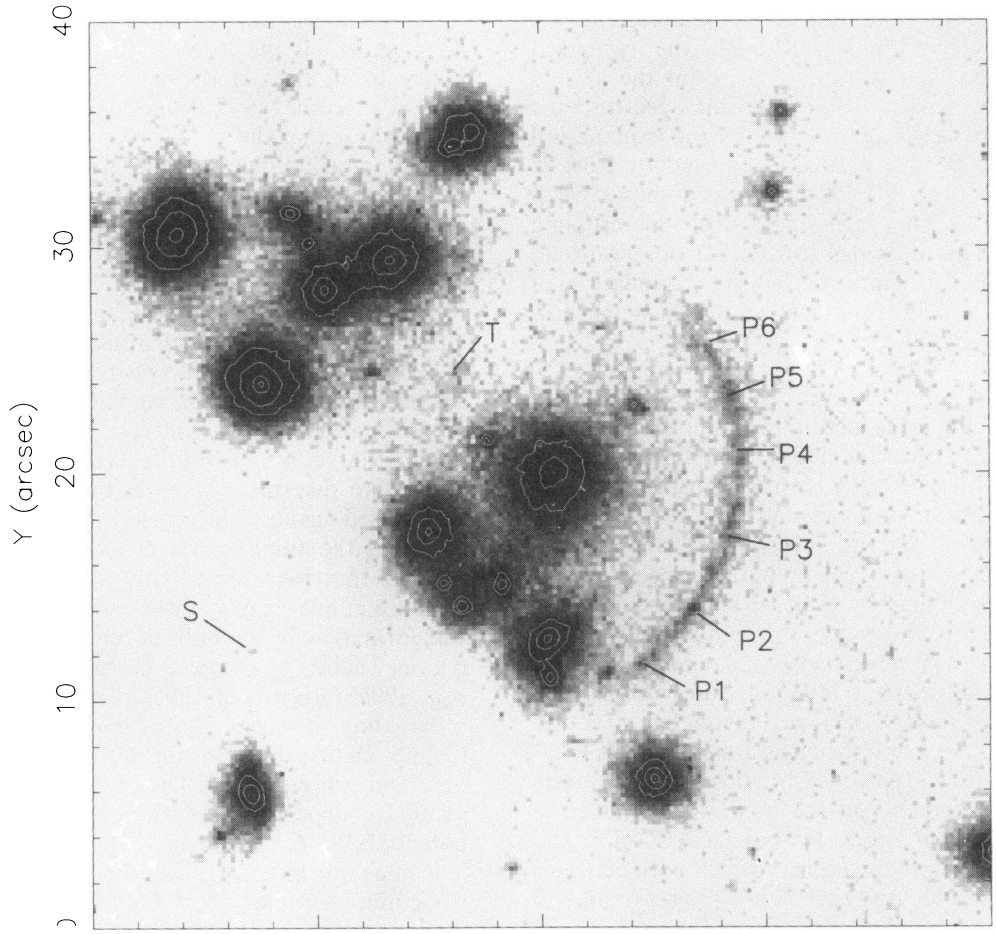

FIG. 4.—The core of the compact cluster Cl 2244−02 at $z_{cl} = 0.33$. The partial Einstein ring is clearly visible, as are various surface brightness peaks along this arc. We use the naming scheme of Hammer et al. (1989) to label these features. The objects S and T were proposed by Hammer et al. (1989) as possible additional images of the background source at $z_{arc} = 2.238$.

surface brightness to the radial arc but smaller angular extent, making them too faint to be detected in the current data. Identification of the other images in deeper *HST* data will constrain strongly the core radius of the mass distribution in this cluster.

3.3. A2218; $z_{cl} = 0.18$

This cluster was first recognized as a strong gravitational lens by Pelló et al. (1988). They subsequently uncovered a large number of candidate arcs and arclets in the cluster core (Pelló et al. 1992) and confirmed spectroscopically two of the brighter candidate arcs. We have followed the naming convention used by Pelló et al. (1992).

Object LPS 289 is a typical very blue, high-redshift arc ($z_{arc} = 1.034$; Fig. 3*a*). The arc lies close to a bright subclump within the cluster, in the saddle between the subclump and the dominant cluster galaxy. The southern end of the arc (section 1, Fig. 3*a*) has high surface brightness, and our WFPC-2 image uncovers a wealth of detail in this feature including a number of bright, unresolved points in a complex pattern, all embedded in a lower surface brightness halo, roughly 7″.5 long. The remainder of the arc (sections 2–3) has much lower surface brightness and also lies in the halo of the subclump. We propose that the arc consists of a singly imaged bright area (section 1) and a fainter region of the source which is multiply imaged (sections 2–3). This configuration is thus very similar to that seen with the arc A0 in A370, although in this case the source morphology appears much less regular.

In contrast to LPS 289, LPS 359 has a very smooth appearance ($z_{arc} = 0.702$, Fig. 3*b*). This arc also differs from LPS 289 in its relatively red colors (Table 2). The main section of the arc is 6″.8 long, and the brightness of this arc and its distance from the cluster center both imply that it is composed of two images of the background source, although no strong break in the light profile is visible (Kneib et al. 1995a, 1995b).

We wish finally to comment on the object LPS 384, for which inconclusive spectroscopy has been obtained. Pelló et al. (1992) present photometry and a low signal-to-noise spectrum of this candidate arc. They conclude that the source is most likely foreground of the cluster and therefore not lensed, although they discuss also the possibility that the object is a very high redshift gravitationally lensed source, $z_{arc} \gtrsim 2.6$. The *HST* image of this object leaves no doubt that it is gravitationally lensed (Fig. 3*c*). The arc is formed by two merging images of the background source, and the parity of the two images is illustrated graphically by the mirrored structures in the two images. These structures allow us to identify unambiguously a third image (LPS 468), which is shown in Figure 3*c*.

In addition to the arcs in this cluster, Pelló et al. (1992) uncovered an unusual ring like feature around one of the cluster galaxies (373, Fig. 3*b*). They suggested that this

might be an Einstein ring, and they were able to recreate the feature under this hypothesis, although the contrived lensing geometry led later groups to discount the lensing model (Kassiola & Kovner 1993). Recent spectroscopic studies also tend to weigh against the lensing explanation for this feature (Le Borgne & Pelló, reported by Fort & Mellier 1994). Our deep WFPC-2 exposure shows weak spiral structure in the ring, including a dust lane crossing the arc LPS 359. This provides substantial observational evidence against the gravitational lensing explanation of this feature, and we conclude that it is a faint red stellar disk associated with LPS 373.

3.4. Cl 2244−02 $z_{cl} = 0.33$

The remarkable circular structure in this cluster was discovered by Lynds & Petrosian (1989) and confirmed spectroscopically as a gravitationally lensed arc using very long integrations and a novel circular spectroscopic slit (Mellier et al. 1991). The redshift determination comes from identification of a line at the extreme blue limit of the spectrograph, assumed to be Lyα giving $z_{arc} = 2.237$. Irrespective of the reality or identification of this line, the continuum shape of the source means it must nevertheless be at relatively high redshift ($z_{arc} \gtrsim 1$). Subsequent imaging observations presented in Hammer et al. (1989) showed distinctive structure within the arc, and we mark their features on the WFC-1 image in Figure 4. The six surface brightness peaks along the arc have been explained in the model of Hammer & Rigaut (1989) as arising from two images (P1–P3 and P4–P6) of a single background source, which itself contains three peaks. They also identify two other possible images of the source: S and T. In this model, the two images P1–P3 and P4–P6 ought to have reversed parities, and this has been confirmed from optical-infrared color gradients (Smail et al. 1993). This study also uncovered in this cluster the first infrared-selected gravitational arc, but unfortunately the current exposure is too short to detect this feature.

In the light of the proposed model of this arc, one feature in the arc bears comment: the relative brightness of P2 compared to the other structures in the arc. The mirror symmetry postulated for the arc is broken by the relative brightness of P2 compared to its mirror image, P5. The peak surface brightness of P2 is a factor of ~ 2 higher than the similar region of P5. Three possible explanations exist for this discrepancy. First, the bright peak may be a superimposed faint star/galaxy, although the similarity of the colors of P2 and P5 means that the additional source must be fairly blue. Secondly, the source seen as P2/P5 may have varied in brightness, which coupled to the different light travel times from the observer to source for the two images would lead to one image being brighter than the other for a period of time. The last possibility is the most interesting; this is that a small region of arc around P2 is being amplified by a superimposed massive dark object within the cluster, as discussed by Fort & Mellier (1994) using their CFHT *B* exposures. New postrefurbishment multicolor observations of this arc are being obtained, and they should determine conclusively the reason for P2's brightness.

4. DISCUSSION

The aim of this study is to gain a first view of the morphologies and sizes of typical star-forming field galaxies at cosmologically interesting look-back times, back to $z \sim 1$–2 or from 8 to 11 Gyr ago (for $h = 0.5$). In particular, we wish to determine (1) the average sizes of high-redshift galaxies, (2) whether all the local galaxy types are present in the high-redshift field, and (3) whether any new populations exist (e.g., Giraud 1992; Miralda-Escudé & Fort 1993).

It is clear that the arc sources demonstrate a wide variation in morphologies (Table 2, Figs. 1–4). The extended sources range from smooth, red systems (e.g., LPS 359 in A2218), through smooth, blue sources (e.g., A5 in A370), to objects with significant internal structure (e.g., Cl 0024+16). These characteristics are very similar to what would be observed if we took a cross section of the local field population, with the obvious identification of star-forming disk systems and smooth red spheroidals. Within the scheme adopted by Giraud (1992), we find that 50% of our spectroscopic sample show evidence for multiple components within the source (Table 2). With our current data, it is difficult to determine whether this reflects substructure in the lensed galaxy or close interactions and mergers, although the small scales probed ($\lesssim 0.5\ h^{-1}$ kpc) would indicate that we are probably seeing individual structures within a single galaxy. Either way, it is apparent that the star formation in the bulk of our sample occurs in distinct regions leading to complex morphologies (e.g., Glazebrook et al. 1996; Driver et al. 1995).

To study the scale sizes of the sources, we must address the possibility that lensing amplification will change the observed source profile. The radial amplification, A_{rad}, of a giant arc depends upon the compactness of the lensing potential (Wu & Hammer 1993). For a lens with an isothermal mass profile ($\Sigma \sim r^{-1}$), the amplification is $A_{rad} = 1$, while more compact mass distributions form narrower arcs ($A_{rad} < 1$) and shallower mass profiles produce thicker arcs ($A_{rad} > 1$). The majority of giant arcs that have been modeled in detail show that the gross properties of the very central regions of the cluster potential can be characterized by a nearly singular isothermal mass distribution with core radii of $\lesssim 25\ h^{-1}$ kpc (e.g., Kneib et al. 1993; Smail et al. 1995b). In this work, we have confirmation of this assumption from the discovery of a candidate radial arc in the well-studied cluster A370. This is only the second such feature discovered, and it illustrates the advantages of working at high spatial resolution when studying lensed features. Furthermore, our modeling of the cluster potential in Cl 0024+16 also indicates a very small core radius for that cluster (see Wallington et al. 1995). This can be confirmed observationally using our prediction that a faint feature in the cluster center is a fifth image of the background source. The presence of such a feature, if associated with the giant arc, is particularly exciting, as this would indicate a compact mass distribution within a cluster that lacks a dominant central galaxy (Miralda-Escudé 1995).

The compactness of the lensing potentials derived above shows that although giant arcs are highly elongated in the tangential direction, we expect the radial magnification to be $A_{rad} \sim 1$ within 10%–20%. Hence, we can adopt the radial light profile of an arc as an unmagnified one-dimensional slice through the source.

The half-light radii for our sample are given in Table 2 and illustrated in Figure 5. We have chosen to compare our sample with spirals, the dominant local population of star-forming galaxies. We use, therefore, a local sample taken from Mathewson et al.'s survey (Mathewson, Ford, & Buchhorn 1992) and a more distant sample analyzed from WFC-1 MDS images by Mutz et al. (1994). The typical

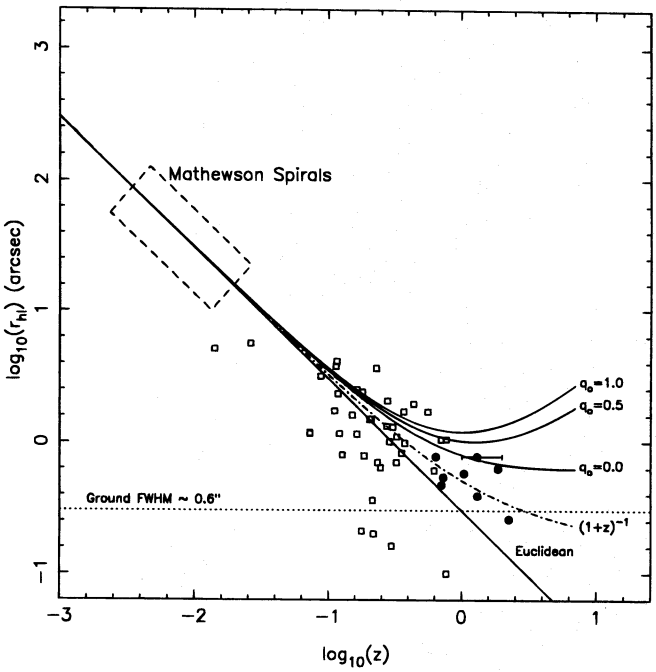

FIG. 5.—The distribution of observed half-light radii vs. redshift for the arc sample (*filled circles*). We assume no radial magnification by the lensing process. We plot for comparison the half-light radii of spiral galaxies from both local (Mathewson et al. 1992) and moderate redshift samples (*open squares*; Mutz et al. 1994). Finally, we show the observed half-light radii of a typical local spiral galaxy, $r_{hl} = 4.4\ h^{-1}$ kpc, as a function of redshift in different cosmologies and the effect of a scale evolution of the form $r_{hl} \propto (1+z)^{-1}$ in a $q_0 = 0.5$ cosmology. The relative dearth of large sources over smaller systems, compared to that expected from a nonevolving population of sources, is readily apparent. This plot is adapted from Mutz et al. (1994).

half-light radius in the Mathewson et al. sample is $r_{hl} \sim 4.4\ h^{-1}$ kpc, equivalent to a scale length of $r_s = 2.7\ h^{-1}$ kpc (Mutz et al. 1994). We plot the variation in apparent angular size of such disks as a function of cosmology in Figure 5.

The observed arc half-light radii follow a smooth progression from the scale lengths observed in the lower redshift samples. However, the distribution of arc half-light radii is apparently incompatible with a nonevolving population of disks with intrinsic half-light radii $r_{hl} \sim 4.4\ h^{-1}$ kpc, irrespective of the adopted geometry. The mean half-light radii of the arc sources is $\langle r_{hl} \rangle = (2.3 \pm 0.8) h^{-1}$ kpc. Thus, the average arc source is a factor of $\sim$1.5–2 times smaller than would have been expected from extrapolation of the r_{hl} of local bright star-forming systems, in standard geometries.

To indicate the strength of evolution required to connect the arc source r_{hl} to local spirals, we plot on Figure 5 a model, $r_{hl} \propto (1+z)^{-1}$, which Mutz et al. (1994) state is consistent with their observations; see also Im et al. (1995). A more detailed comparison with the Mutz et al. (1994) sample is hampered by the small samples, but what is apparent, however, is the absence of the larger sources ($r_{hl} \gtrsim 5\ h^{-1}$ kpc) relative to smaller sources in the arc catalog. As we discussed earlier, this cannot be explained by selection effects in the original sample, and we must therefore accept that either (1) large galaxies with very extended star-forming regions are rarer at $z \sim 1$–2 than they are today, or (2) the relative proportions of large and small galaxies has changed between $z \sim 1$ and today. The small number of giant arcs precludes us from distinguishing between these alternatives. However, the latter possibility is discussed at length in Driver et al. (1995) and Glazebrook et al. (1996).

These conclusions are similar to those reached by Smail et al. (1993), who used K imaging of a sample of giant arcs, which overlaps considerably that used here, to measure the rest-frame near-infrared luminosities of the sources. They found that the arc sources had sub-K^* luminosities compared to the local field. This result could arise from either a lack of massive, luminous galaxies at $z \gtrsim 1$, or an increase in the relative abundance of dwarf galaxies compared to more massive systems. Thus, the distributions of both K luminosities and sizes of $z \gtrsim 1$ field galaxies indicate that dominance of large, massive galaxies is a relatively recent feature of the field population.

The power of using arcs and arclets for studying the evolution of the sizes of faint galaxies comes from the large redshift range probed. As Kneib et al. (1995b) show, it is possible, using *HST* observations of a well-constrained lensing cluster, to study the redshift distribution of very faint galaxies, $R \lesssim 26$–27, from the shear induced in the galaxy images by the cluster. In principle, with deep enough data this technique can be extended to study the distribution of scale sizes as a function of redshift for large samples of very faint galaxies, well beyond the reach of conventional spectroscopy.

5. CONCLUSIONS

1. We have analyzed deep pre- and postrefurbishment images of eight spectroscopically confirmed giant arcs, arclets, and pairs to study the morphologies and sizes of typical galaxies in the $z \sim 1$ field population.

2. In addition, our high-resolution imaging has enabled us to improve the mass models of two of our clusters, Cl 0024+16 and A370, from modeling of multiply imaged background sources and the identification of candidate arcs in the cores of both clusters. Both models indicate very compact, $r_c \sim 25\ h^{-1}$ kpc, mass distributions in these clusters, in agreement with the limits derived by other workers. However, the result for Cl 0024+16 is particularly interesting, as this cluster lacks a single central dominant galaxy.

3. We suggest that star-forming galaxies at high redshift are considerably ($\sim$1.5–2 times) more compact than the bright star-forming spiral galaxies that dominate the local field population. We have argued that the obvious selection effects in the sample would tend to bias us against finding "thin" arcs, and thus the observed trend to smaller scale sizes in the admittedly small sample of giant arcs is interesting. If the arc sources are precursors of the local, bright spiral population, then this result argues for evolution in the disk sizes over the last $\sim$10 Gyr. A similar conclusion was drawn from near-infrared imaging of the giant arcs, which showed that the bulk of the $z \gtrsim 1$ sources are sub-L^* compared to the local field (Smail et al. 1993). Both these results can be explained by either an absence of large galaxies from the $z \sim 1$ field population or a shift in the ratio of massive/dwarf galaxies. Either possibility indicates a considerable change in the nature of the field population, since $z \sim 1$.

4. At the moment, this technique is limited by the small sample of giant arcs available. This obstacle can be removed by using very deep *HST* imaging of a number of well-constrained lensing clusters. The large samples of arclets

produced can be analyzed to provide both the redshift and scale size information needed to tackle conclusively the question of the size evolution of "normal" galaxies at high redshift.

We thank the referee, E. Falco, for many helpful comments on this paper. We also wish to thank S. Mutz for providing the data from his *HST* study. Finally, we thank Roger Blandford, Bernard Fort, David Hogg, Yannick Mellier, and Jordi Miralda-Escudé for useful discussions. Support via a NATO Advanced Fellowship and a Carnegie Fellowship (I. R. S.) and an EC Fellowship (J-P. K.) are gratefully acknowledged. W. J. C. acknowledges support from the Australian Department of Industry, Science and Technology, the Australian Research Council, and Sun Microsystems.

REFERENCES

Aragón-Salamanca, A., & Ellis, R. S. 1990, in Gravitational Lensing, ed. Y. Mellier, G. Soucail, & B. Fort (Berlin: Springer-Verlag), 288
Couch, W. J., Ellis, R. S., Sharples, R. M., & Smail, I. 1994, ApJ, 430, 121
Dressler, A., Oemler, A., Butcher, H., & Gunn, J. E. 1994, ApJ, 430, 107
Driver, S. P., Windhorst, R. A., Ostrander, E. J., Keel, W. C., Griffiths, R. E., & Ratnatunga, K. U. 1995, ApJ, 449, L23
Ellis, R. S. 1994, in IAU Symp. 164, Stellar Populations, ed. P. van der Kruit & G. Gilmore (Dordrecht: Kluwer)
Fort, B., & Mellier, Y. 1994, A&A, Rev., 5, 239
Fort, B., Prieur, J.-L., Mathez, G., Mellier, Y., & Soucail, G. 1988, A&A, 200, 17
Giraud, E. 1992, A&A, 257, 501
Glazebrook, K., Ellis, R. S., Colless, M. M., Broadhurst, T. J., Allington-Smith, J., & Tanvir, N. R. 1995, MNRAS, 273, 157
Glazebrook, K., Ellis, R. S., Santiago, B., & Griffiths, R. E. 1996, MNRAS, in press
Hammer, F., Le Fevre, O., Jones, J., Rigaut, F., & Soucail, G. 1989, A&A, 208, L7
Hammer, F., & Rigaut, F. 1989, A&A, 226, 45
Im, M., Casertano, S., Griffiths, R. E., & Ratnatunga, K. U. 1996, ApJ, in press
Kassiola, A., & Kovner, I. 1993, ApJ, 417, 474
Kassiola, A., Kovner, I., & Dantel-Fort, M. 1995, MNRAS, submitted
Kassiola, A., Kovner, I., & Fort, B. 1992, ApJ, 400, 41
Kassiola, A., Kovner, I., Fort, B., & Mellier, Y. 1994, ApJ, 429, L9
Kneib, J.-P., Ellis, R. S., Smail, I., Couch, W. J., & Sharples, R. M. 1995b, ApJ, submitted
Kneib, J.-P., Mathez, G., Fort, B., Mellier, Y., & Soucail, G. 1994, A&A, 286, 701
Kneib, J.-P., Mellier, Y., Fort, B., & Mathez, G. 1993, A&A, 273, 367
Kneib, J.-P., Mellier, Y., Pelló, R., Miralda-Escudé, J., Le Borgne, J.-F., Böhringer, H., & Picat, J.-P. 1995a, A&A, 303, 27
Koo, D. C. 1988, in Large-Scale Motions in the Universe, ed. V. G. Rubin & G. V. Cayne (Princeton: Princeton Univ. Press), 513
Krist, J. 1992, TINYTIM User's Manual (Baltimore: STScI)
Lilly, S. L. 1993, ApJ, 411, 501
Lynds, R., & Petrosian, V. 1989, ApJ, 336, 1
Mathewson, D. S., Ford, V. L., & Buchhorn, M. 1992, ApJS, 81, 413
Mellier, Y., Fort, B., & Kneib, J.-P. 1993, ApJ, 407, 33
Mellier, Y., Fort, B., Soucail, G., Mathez, G., & Cailloux, M. 1991, ApJ, 380, 334
Miralda-Escudé, J. 1995, ApJ, 438, 514
Miralda-Escudé, J., & Fort, B. 1993, ApJ, 417, L5
Mutz, S. B., et al. 1994, ApJ, 434, L55
Pelló, R., Le Borgne, J. F., Sanahuja, B., Mathez, G., & Fort, B. 1988, A&A, 190, L11
———. 1992, A&A, 266, 6
Smail, I., Couch, W. J., Ellis, R. S., & Sharples, R. M. 1995a, ApJ, 440, 501
Smail, I., Ellis, R. S., Aragòn-Salamanca, A., Soucail, G., Mellier, Y., & Giraud, E. 1993, MNRAS, 263, 628
Smail, I., Ellis, R. S., & Fitchett, M. J. 1994, MNRAS, 270, 245
Smail, I., Hogg, D. W., Blandford, R. D., Cohen, J. G., Edge, A. C., & Djorgovski, S. G. 1995b, MNRAS, 277, 16
Tresse, L., Hammer, F., Le Fevre, O., & Proust, D. 1993, A&A, 277, 53
Wallington, S., Kochanek, C. S., & Koo, D. C. 1995, ApJ, 441, 58
Windhorst, R. A., et al. 1994, AJ, 107, 930
Wu, X. P., & Hammer, F. 1993, MNRAS, 262, 187